Long-term evolution of acinar-to-ductal metaplasia and β-cell mass after radiofrequency-assisted transection of the pancreas in a controlled large animal model

Rita Quesada [1], Anna Andaluz [2], Marta Cáceres [3], Xavier Moll [2], Mar Iglesias [4], Dimitri Dorcaratto[5], Ignasi Poves [6], Enrique Berjano [7], Luis Grande[6], Fernando Burdío [6].

[1] Cancer Research Group HBP, Fundación Instituto Mar de Investigaciones Médicas, Doctor Aiguader 88, Barcelona 08003, Spain

[2]Medicine and Surgery of Animals Department, Facultat de Veterinària, Universitat Autònoma de Barcelona, Bellaterra, Barcelona 08193, Spain.

[3] General and Digestive Surgery Department, Hospital Universitari Sagrat cor, Viladomat 288, 08029 Barcelona, Spain

[4] Department of Pathology, Hospital del Mar, Passeig Marítim 25-29, Barcelona 08003, Spain

[5] Hepatobiliary and Liver Transplant Surgical Unit, St. Vincent's University Hospital, Elm Park, Dublin 4, Ireland

[6] General Surgery Department, Hospital del Mar, Passeig Marítim 25-29, Barcelona 08003, Spain.

[7] Biomedical Synergy, Electronic Engineering Department, Universitat Politècnica de València, Valencia 46022, Spain.

Short title: Histological evalution of a RF-assisted transection of the pancreas

Key words: Acinar-to-ductal metaplasia; Duodenopancreatectomy; Radiofrequency-assisted transection; animal model

Full Address:

Corresponding author and person to whom reprints requests should be addressed:

Rita Quesada, PhD

Fundación Instituto Mar de Investigaciones Médicas (Fundación IMIM)

Cancer Research Group HBP

Doctor Aiguader 88,

Barcelona 08003, Spain.

Fax: + 34 93 316 16 21. E-mail: rita.quesada.di@gmail.com

ABSTRACT:

Background: Pancreatic duct ligation (PDL) has been used as a model of chronic pancreatitis and as a model to increase β-cell mass. However, studies in mice have demonstrated acinar regeneration after PDL, questioning the long-term validity of the model. We aim to elucidate whether RF-assisted transection (RFAT) of the main pancreatic duct is a reliable PDL model, both in short (ST, 1-month) and long-term (LT, 6-months) follow-ups. Methods: Eleven pigs were subjected to RFAT. Biochemical (serum/peripancreatic amylase and glucose) and histological changes (including a semiautomatic morphometric study of over 1000 images/pancreas and IHC analysis) were evaluated after ST or LT follow-up and also in fresh pancreas specimens that were used as controls for 1 (n=4) and 6 months (n=6). Results: The distal pancreas in the ST was characterized by areas of acinar-to-ductal metaplasia (56%) which were significantly reduced at LT (21%) by fibrotic replacement and adipose tissue. The endocrine mass showed a normal increase. Conclusion: RFAT in the pig seems to be an appropriate PDL model without restoration of pancreatic drainage or reduction of endocrine mass.

INTRODUCTION

The conversion of exocrine acinar tissue into tubular or ductal complexes, usually known as acinar-to-ductal metaplasia (ADM), is common in various pancreatic diseases including pancreatitis and cancer [1–3]. Since ADM is characterized by a switch from acinar to ductal phenotype with active proliferation, and since metaplasic ductal lesions are frequently seen in chronic pancreatitis as well as in specimens of pancreatic ductal adenocarcinoma (PDAC), ADM is thought to represent a preneoplastic condition [1,3,4]. Even though some areas of ADM could revert to normal acinar morphology [5,6] in the absence of oncogenic Kras mutations or in the presence of acute pancreatitis, the transition of acinar cells into a duct-like state (as in ADM) has been recognized as an important early event in tumor initiation.

Pancreatic duct ligation (PDL) in mouse models has been extensively used as a model of chronic pancreatitis in order to study the evolution of ADM into PDAC [1,3,7], and also as a model of duct-to-islet differentiation [6,8–12] to increase beta-cell mass. However, the validity of PDL as a model of endocrine regeneration has now been called into question [5–7,11,13,14]. Recent results from PDL in mouse models have shown that some acinar cells can escape death [7] and that acinar compartment can regenerate in a long-term evolution after PDL (over 6 months), probably by restoration of pancreatic drainage [6]. Ever since the first studies on PDL in mouse models it has been said that this technique is difficult because its unique anatomy hampers the results [15,16]. The mouse pancreas is usually poorly defined and consists of three lobes (gastric, splenic and duodenal) which drain their juices via individual ducts only 150 μm in diameter [16,17] and there are also frequent variations in this drainage. Researchers usually ligate the splenic lobe from the rest of the pancreas, however this technique is challenging due to the small diameter of the pancreatic duct and usually requires the help of a microscope for the dissection. Many of these anatomical difficulties can be overcome with a large pancreas model, such as the pig model, in which the pancreas is large and clearly defined [18], especially if the closed proximal part (duodenal lobe) is preserved to avoid a difficult-to-treat steatorrhea [19]. However, in the pig model a larger amount of tissue must be severed and hence PDL may not be able to avoid a pancreatic fistula or to efficiently occlude the main pancreatic duct in the mid pancreas.

Radiofrequency (RF) energy has been used both experimentally and clinically to manage the pancreatic remnant after distal pancreatectomies to seal the main and secondary pancreatic ducts [20–22]. In recent years, our group has tested the ability of some RF electrodes to seal vessels in the liver [23,24]

and kidney [25]. A recent study conducted on a porcine pancreatic model suggested that distal pancreatic transection by RF electrode can seal the main pancreatic duct easily and safely [22]. We have also demonstrated in a rat model that RF-assisted transection of the neck of the pancreas may safely seal the remnant distal pancreas and activate a rapid and massive exocrine atrophy without leading to necrotizing pancreatitis [12]. We therefore hypothesized that this technique could be used to occlude pancreatic ducts while severing large amounts of tissue, as in the mid pancreas of large animals.

With the above considerations in mind, the aim of this study was to elucidate whether RF-assisted transection (RFAT) of the main pancreatic duct in the mid porcine pancreas would be a reliable PDL model over a follow up period of 6 months. This technique could avoid both exocrine insufficiency and fistula formation without the risk of restoring pancreatic drainage.

METHODS

Study design and Animal model

A total of 11 Landrace pigs were subjected to RFAT of the neck of the pancreas with different survival periods: Groups “Exp-1-month” (n=6) and “Exp-6-months” (n=5) with 1 and 6 months postoperative period (PO), respectively. Additionally, fresh pancreatic specimens from animals weighing 40 kg (“Control-1-month”, n=4) and 120 kg (“Control-6-months”, n=6) were used as controls for 1 and 6 months, respectively. The study was conducted according to the guidelines approved by the Government of Catalonia’s Animal Care Committee and as described in [22].

Surgical technique

Preoperative, anaesthesia and postoperative care was provided by fully trained veterinary staff members as described in [22]. In order to achieve complete obstruction of the distal part (body and tail) of the pancreatic gland was transected including the main pancreatic duct which was severed over and below the portal vein according to the previous study on pancreas anatomy (Figure 1) [18]. The pancreas was mobilized and slightly tractioned to ensure a 5-mm minimum safe distance between RFAT site and major peripancreatic vessels and surrounding viscera to avoid unexpected injuries. The main pancreatic duct was neither identified nor sutured after transection. The transection was performed using a RF-assisted device (Coolinside, Apeiron Medical, Valencia, Spain) [12,22] and a silicon drain was positioned adjacent to the pancreatic stump.

Necropsy

One and six months after the initial procedure all animals were again anesthetized, intubated and ventilated as described in [22]. Exploratory laparotomy was performed and the peritoneal cavity was assessed at necropsy. The pancreatic stump was skeletonized, photographed and the proximal and distal pancreas were dissected, removed and placed in 10% paraformaldehyde for further histopathologic processing. The animals were then sacrificed with a commercial euthanasia solution.

Laboratory measurements

Serum amylase and glucose levels were obtained prior to the surgical procedure, 4 hours after intervention, on days 3, 7, 15, 21 and 1 or 6 months PO before euthanasia. Peripancreatic fluid amylase concentrations were measured during laparotomy, from the drain tube on Day 3 and at necropsy. The surgical drain was retired in all the animals on Day 3 PO, because the output was <20 ml per day.

Histopathologic study

The histopathologic analysis was performed on three different slices of the pancreas. One slice of the proximal pancreas at 4 cm from the area of transection (PP) and two in the distal pancreas (DP): 1 cm next to the transection area (D1) and another before the tail (D2) (Figure 2A-1).

Fixed samples were embedded in paraffin, cut (3 μm) and stained with hematoxylin-eosin to assess histological changes and also Masson's Trichrome to observe collagen fibers. To evaluate apoptotic response, endocrine function and ADM immunohistochemical analysis, consecutive slices of the distal and proximal pancreas were incubated with primary antibodies: rabbit anti-cleaved caspase-3 (K3, 1:1600; Cell Signalling Technology), rabbit anti-insulin (I, 1:400, Cell Signalling Technology) and mouse anti-cytokeratin-7 (Ck7, 1:120, Santa Cruz Biotechnology), respectively. The secondary antibody was an avidin-biotin complex-conjugated solution of Real DAKO (EnVision, Copenhagen, Denmark). The proximal pancreas was used as a control of normal pancreatic tissue within subjects.

Morphometric analysis

"The morphometric results of the distal part were expressed separately for D1 and D2, but hereinafter the mean value is referred as DP.

Automatic acquisitions of consecutive immunohistochemistry stained slices of Ck7 and I were performed with a DMI-6000B Leica microscope (Leica Microsystems, Wetzlar, Germany) and Micro–

manager software (www.micro-manager.org, San Francisco) to quantify histological changes. A FIJI macro was conducted to analyze: the mean area of Ck7 expression (MA-Ck7, expressed in μm^2), the mean area of insulin expression (MA-I, expressed in μm^2) and the average size of islets (μm^2) (Figure 2A-2). To adjust the staining variability, random captures of each acquisition were used to adjust hue, saturation and brightness, after which the segmentation algorithm for particle detection was applied. A segmentation process was performed on macroscopic images of the slices by 3D-DOCTOR software (Able Software Corp, Lexington, MA, USA) to evaluate the cross-sectional area of pancreas, differentiating the adipose/connective tissue, the area of pancreatic parenchyma (which excluded the connective capsule of the pancreas, ductal dilatation and the adipose tissue) or ADM (Figure 2A-3).

Statistical analysis

Kolmogorov–Smirnov Test followed by a Student's t-Test or U Mann-Whitney Test for nonparametric data was performed by SPSS software. The laboratory analyses that included repeated measures were evaluated by the Bonferroni Test for post hoc analysis. Data were expressed as means ± SEM and we considered a value of $p<0.05$ to be statistically significant.

RESULTS

Intraoperative features and postoperative follow-up

All the animals tolerated the surgical procedure well and quickly recovered and ambulated, tolerating the intake without signs of relevant pancreatic disease. The animals showed a normal growth curve (preoperatively and pre-necropsy at 1 and 6 months, 26±8 kg, 39±12 kg and 125±14 kg, respectively).

Laboratory analysis

All the animals showed a significant increase of amylase levels ($p<0.05$) in both serum (4^{th} hour PO and 3^{rd} day PO) and peritoneum (3^{rd} day PO), which returned to baseline levels on the following days, as previously observed in the literature [12,22] (Table 1). No animals presented any postoperative clinical complication or free intraabdominal fluid at necropsy, neither at 1 or 6 months.

Histopathological and morphometric study

The histopathological study of the transection margin of the pancreas stump in the Exp-1-month group, showed a common pattern of coagulative necrosis surrounded by an intense fibrotic component which was totally replaced by fibrotic tissue in Exp-6-months. The fibrosis reaction also completely encircled the main and secondary pancreatic ducts, as previously described in [22].

No differences were observed between the morphometric results of D1 and D2. MA-Ck7 was significantly greater in DP (6.4±0.9 mm^2) than PP for group Exp-1-month (4.2±0.7 mm^2), which correlated histologically with areas of ADM. At 6 months PO, there was an increase of MA-Ck7 in group Control-6-months and in the PP of the animals subjected to the RFAT, while there was a significant decrease in MA-Ck7 in the DP (3.1±0.5 mm^2) of the Exp-6-months (Figures 2-B and 3 g-i) compared to Exp-1-month, which was also correlated histologically with an increase in fibrotic tissue and a decrease in ADM areas (Figure 3 m-o). There was no evidence of significant caspase-3 activity in any of the pancreatic areas (Figure 3 d-f).

Concerning the endocrine tissue, MA-I was considerably higher at 6 months than at 1 month, with no differences between groups, either in PP and DP or between controls and experimental groups (Figure 2-C). Mean islet size (Figure 2-D) also showed a progressive increase in controls and in PP of the RFAT group with growth of the animal. However, mean islet size of the DP in group Exp-6-months was significantly lower (446±108 μm^2) than the PP in the same group. Mean islet size of DP in group Exp-6-months was even lower than in Exp-1-month (780±74 μm^2) and also lower than islet size in the DP in Control-6-months (729±149 μm^2). These results were histologically consistent with a significant increase in small isolated clusters of β-cells in DP of the Exp-6-months (Figures 2-D2 and D3). The increase in these isolated endocrine cells led to a decrease in mean islet size, though macro islets of equal size were also identified in the proximal pancreas.

As the animals increased in size, we observed an increase in the cross-sectional area of pancreas without significant differences between the distal and the proximal pancreas (Figure 2-E). The area of the pancreatic parenchyma increased proportionally to the cross-sectional area of the pancreas in control specimens and in the PP of the animals subjected to RFAT. As expected, the DP at Exp-1-month was characterized by an increase in ADM (reaching 56% of the cross-sectional area at this time) with no evidence of preserved pancreatic parenchyma. However, this area of ADM was reduced from 1.5 ± 0.2 cm^2 at 1 month to 1.2 ± 0.2 cm^2 at 6 months, in spite of the growth of the animal, and was only 21% of

the distal cross-sectional pancreatic area at Exp-6-months. There were no significant differences between the mean area of connective and adipose tissue in DP and PP in the control specimens. In contrast, an increase of the adipose and connective tissue was observed over the PO period in proximal and distal pancreas of the animals subjected to RFAT. This increase was especially significant in the DP at Exp-6-months (80% of the cross-sectional area).

DISCUSSION

PDL has been extensively used to study the conversion of ADM into PDAC [1,3] as well as a method of duct-to-islet differentiation [6,8–12] in order to increase beta-cell mass. However, contradictory results have been obtained from the conventional mouse models [6,7,11,26].

Since complete duct occlusion should prevent duct cells regenerating into acinar cells after PDL [16] and some morphometric results could have been biased by including injured pancreas [7,11], the present study implemented six key differences from conventional PDL mouse models in order to ensure efficient and reliable pancreatic duct occlusion and accurate evaluation:

To start with, large animal model are used with a well-defined pancreas anatomy, and hence easy-to-manipulate and identify, as well as being more similar to human specimens, which facilitates clinical translation. Secondly, we considered short (1 month PO) and long-term (6 months PO) evolution study of both ADM and β-cell mass, which is especially relevant since the vast majority of studies on ADM after PDL are restricted to short-term. Additionally, two control groups (non-PDL animals) of similar age and size (with survival periods equal to the experimental groups) have been used in order compare the histological response with healthy models. To further avoid possible restoration of pancreatic drainage in long-term evolution and preservation of enough tissue in the head of the pancreas to avoid cumbersome esteatorrea and weight loss [19] we performed complete transection of the pancreas. It is also important to highlight that an automatic acquisition of complete pancreatic sections of both Ck7 and insulin expression, including the analysis of up to 1,000 histological photographs per animal was considered to represent the entire pancreas volume. And this analysis is in clear contrast to other manual volumetry calculations which include only selected areas of the preparations [8,16]. Finally, we used a new PDL system based on RF-assisted transection (RFAT) which has previously been shown to avoid pancreatic fistula formation [22,27].

This model has also demonstrated a complete acinar cell deletion in short and long-term evolution with no evidence of acinar compartment regeneration. These results are in contrast to other mouse models [6,7] and even pig models with simple ligation of the main pancreatic duct close to the duodenum –likely because of possible accessory drainages- [19,28,29] in which some regeneration of acinar tissue occurred. Although, the model results in the appearance of ADM in the short term RFAT group, as described after PDL [12,16,30], we have demonstrated the reduction of the ADM area in the long-term group compared to the short-term group (from 56% to 21% of the cross-sectional area), in spite of the growth of the animal. To our knowledge, this issue has not been demonstrated before and may consistently show that ADM may disappear after a reliable obstruction of the pancreatic duct in healthy conditions, as demonstrated by a 3-fold increase in mean preoperative weight. This is in contrast to other mouse and pig models in which the animals usually lost a great deal of weight even in the short term [19]. Also, instead of complete and persistent acinar cell disappearance, there is a normal increase of β-cell mass as the animal grows, which is unaltered in this PDL model. These findings are similar to those found by Rankin *et al.* [11], who demonstrated that β-cell mass and insulin contents were not altered by PDL after a morphometric study of the entire pancreas. Although Xu *et al.* [26] demonstrated a 2-fold post-PDL β-cell expansion that plateaued within 7 days, their results were queried by other authors [11], who considered that their measurements could be biased by the reduced size of the injured pancreas.

In view of the results obtained in this study, we believe that RFAT in the pig seems to be an appropriate PDL model without restoration of pancreatic drainage or reduction of endocrine mass. However, further experimental studies are needed to confirm these results.

Acknowledgements and disclosure statement: “This work was supported by the Spanish "Plan Estatal de Investigación, Desarrollo e Innovación Orientada a los Retos de la Sociedad" under Grant TEC2014-52383-C3 (TEC2014-52383-C3-3-R). RQ, EB, FB declare stock ownership in Apeiron Medical S.L., a company that has a license for the patent US 8.303.584.B2, on which the device have been employed.

REFERENCES

[1] Prévot P-P, Simion A, Grimont A, Colletti M, Khalaileh A, Van den Steen G, et al. Role of the ductal transcription factors HNF6 and Sox9 in pancreatic acinar-to-ductal metaplasia. Gut 2012;61:1723–32.

[2] Lardon J, Bouwens L. Metaplasia in the pancreas. Differentiation 2005;73:278–86.

[3] Martínez-Romero C, Rooman I, Skoudy A, Guerra C, Molero X, González A, et al. The epigenetic regulators Bmi1 and Ring1B are differentially regulated in pancreatitis and pancreatic ductal adenocarcinoma. J Pathol 2009;219:205–13..

[4] Strobel O, Dor Y, Alsina J, Stirman A, Lauwers G, Trainor A, et al. In vivo lineage tracing defines the role of acinar-to-ductal transdifferentiation in inflammatory ductal metaplasia. Gastroenterology 2007;133:1999–2009.

[5] Kopp JL, von Figura G, Mayes E, Liu F-F, Dubois CL, Morris IV john P, et al. Identification of Sox9-dependent acinar-to-ductal reprogramming as the principal mechanism for initiation of pancreatic ductal adenocarcinoma. Cancer Cell 2012;22:737–50.

[6] Cavelti-Weder C, Shtessel M, Reuss JE, Jermendy A, Yamada T, Caballero F, et al. Pancreatic duct ligation after almost complete β-cell loss: exocrine regeneration but no evidence of β-cell regeneration. Endocrinology 2013;154:4493–502.

[7] Van de Casteele M, Leuckx G, Cai Y, Yuchi Y, Coppens V, De Groef S, et al. Partial duct ligation: β-cell proliferation and beyond. Diabetes 2014;63:2567–77.

[8] Wang RN, Klöppel G, Bouwens L. Duct- to islet-cell differentiation and islet growth in the pancreas of duct-ligated adult rats. Diabetologia 1995;38:1405–11.

[9] Li M, Miyagawa J, Moriwaki M, Yuan M, Yang Q, Kozawa J, et al. Analysis of expression profiles of islet-associated transcription and growth factors during beta-cell neogenesis from duct cells in partially duct-ligated mice. Pancreas 2003;27:345–55.

[10] Criscimanna A, Speicher J a, Houshmand G, Shiota C, Prasadan K, Ji B, et al. Duct cells contribute to regeneration of endocrine and acinar cells following pancreatic damage in adult mice. Gastroenterology 2011;141:1451–62, 1462.e1–6.

[11] Rankin MM, Wilbur CJ, Rak K, Shields EJ, Granger A, Kushner JA. beta-Cells are not generated in pancreatic duct ligation-induced injury in adult mice. Diabetes 2013;62:1634–45.

[12] Quesada R, Burdío F, Iglesias M, Dorcaratto D, Cáceres M, Andaluz A, et al. Radiofrequency Pancreatic Ablation and Section of the Main Pancreatic Duct Does Not Lead to Necrotizing Pancreatitis. Pancreas 2014;43:1–7.

[13] Chintinne M, Stangé G, Denys B, Ling Z, In ’t Veld P, Pipeleers D. Beta cell count instead of beta cell mass to assess and localize growth in beta cell population following pancreatic duct ligation in mice. PLoS One 2012;7:e43959.

[14] Xiao X, Chen Z, Shiota C, Prasadan K, Guo P, El-Gohary Y, et al. No evidence for ?? cell neogenesis in murine adult pancreas. J Clin Invest 2013;123:2207–17.

[15] Yang L, Leach SD, Scoggins CR, Meszoely IM, Wada M, Means AL, et al. proliferation in duct-ligated murine pancreas p53-Dependent acinar cell apoptosis triggers epithelial. Am J Physiol Gastrointest Liver Physiol 2000;279:827–36.

[16] Watanabe S, Abe K, Anbo Y, Katoh H. Changes in the mouse exocrine pancreas after pancreatic duct ligation: a qualitative and quantitative histological study. Arch Histol Cytol 1995;58:365–74.

[17] Aghdassi AA, Mayerle J, Christochowitz S, Weiss FU, Sendler M, Lerch MM. Animal models for investigating chronic pancreatitis. Fibrogenesis Tissue Repair 2011;4:26.

[18] Ferrer J, Iii WES, Weegman BP, Suszynski TM, David ER. NIH Public Access. Transplantation 2008;86:1503–10.

[19] Pitkäranta P, Kivisaari L, Nordling S, Saari A, Schröder T. Experimental chronic pancreatitis in the pig. Scand J Gastroenterol 1989;24:987–92. doi:10.3109/00365528909089245.

[20] Blansfield JA, Rapp MM, Chokshi RJ, Woll NL, Hunsinger MA, Sheldon DG, et al. Novel Method of Stump Closure for Distal Pancreatectomy with a 75% Reduction in Pancreatic Fistula Rate. J Gastrointest Surg 2012;16:524–8.

[21] Nagakawa Y, Tsuchida A, Saito H, Tohyama Y, Matsudo T, Kawakita H, et al. The VIO soft-coagulation system can prevent pancreatic fistula following pancreatectomy. J Hepatobiliary Pancreat Surg 2008;15:359–65.

[22] Dorcaratto D, Burdío F, Fondevila D, Andaluz A, Quesada R, Poves I, et al. Radiofrequency is a secure and effective method for pancreatic transection in laparoscopic distal pancreatectomy: results of a randomized, controlled trial in an experimental model. Surg Endosc 2013;27:3710–9.

[23] Burdo F, Grande L, Berjano E, Martinez-Serrano M, Poves I, Burdo JM, et al. A new single-instrument technique for parenchyma division and hemostasis in liver resection: A clinical feasibility study. Am J Surg 2010;200:e75–80.

[24] Navarro A, Burdio F, Berjano EJ, Güemes A, Sousa R, Rufas M, et al. Laparoscopic blood-saving liver resection using a new radiofrequency-assisted device: preliminary report of an in vivo study with pig liver. Surg Endosc 2008;22:1384–91.

[25] Ríos JS, Zalabardo JMS, Burdio F, Berjano E, Moros M, Gonzalez A, et al. Single instrument for hemostatic control in laparoscopic partial nephrectomy in a porcine model without renal vascular clamping. J Endourol 2011;25:1005–11.

[26] Xu X, D'Hoker J, Stangé G, Bonné S, De Leu N, Xiao X, et al. Beta cells can be generated from endogenous progenitors in injured adult mouse pancreas. Cell 2008;132:197–207.

[27] Truty MJ, Sawyer MD, Que FG. Decreasing pancreatic leak after distal pancreatectomy: saline-coupled radiofrequency ablation in a porcine model. J Gastrointest Surg 2007;11:998–1007.

[28] Boerma D, Straatsburg IH, Offerhaus GJA, Gouma DJ, van Gulik TM. Experimental model of obstructive, chronic pancreatitis in pigs. Dig Surg 2003;20:520–6.

[29] Lamme B, Boermeester MA, Straatsburg IH, van Buijtenen JM, Boerma D, Offerhaus GJA, et al. Early versus late surgical drainage for obstructive pancreatitis in an experimental model. Br J Surg 2007;94:849–54.

[30] Walker NI. Ultrastructure of the rat pancreas after experimental duct ligation. I. The role of apoptosis and intraepithelial macrophages in acinar cell deletion. Am J Pathol 1987;126:439–51.

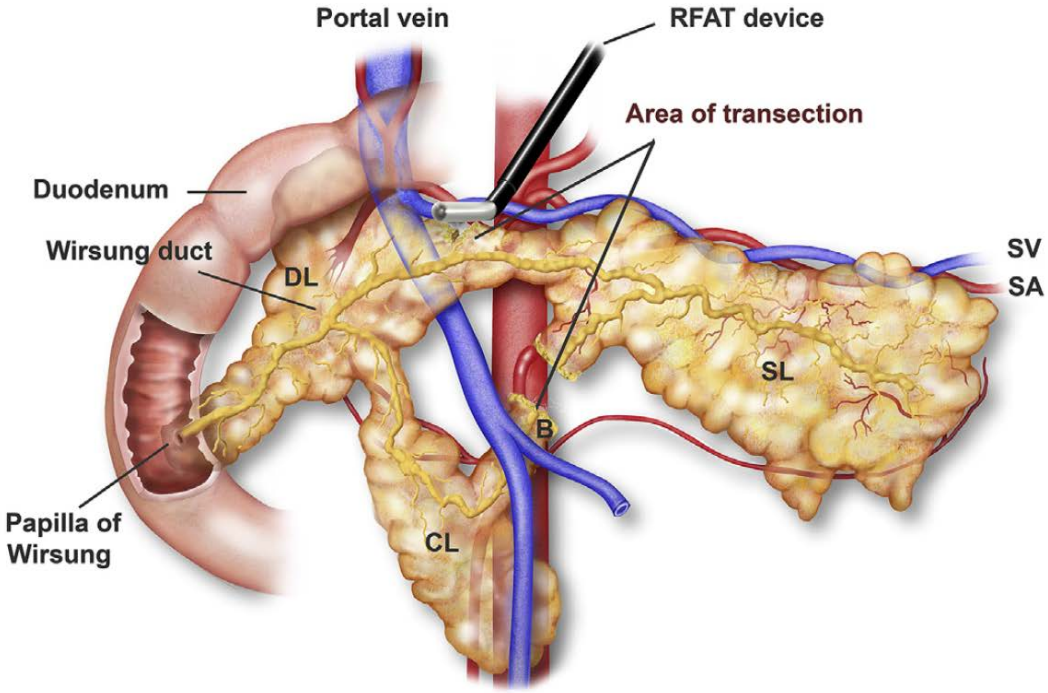

Figure 1: Original illustration of a normal anatomy of the porcine pancreas and the surgical procedure after the first section of the pancreas according to the anatomy described by Ferrer *et al.* [18]. The "splenic" lobe (SL), corresponding to the tail and body in the human pancreas, is attached to the spleen. The "duodenal" lobe (DL), corresponding to the head of the pancreas, is adjacent to the duodenum, while the "connecting" lobe (CL), corresponding to the uncinated process is an extension of the pancreas which is anterior to the portal vein. There is also a "bridge" (B) of pancreatic tissue serving as an anatomical connection between the splenic and connecting lobes behind the portal vein. In order to achieve complete obstruction of the distal part (body and tail) of the pancreas, two sections were performed with the radiofrequency-assisted device.

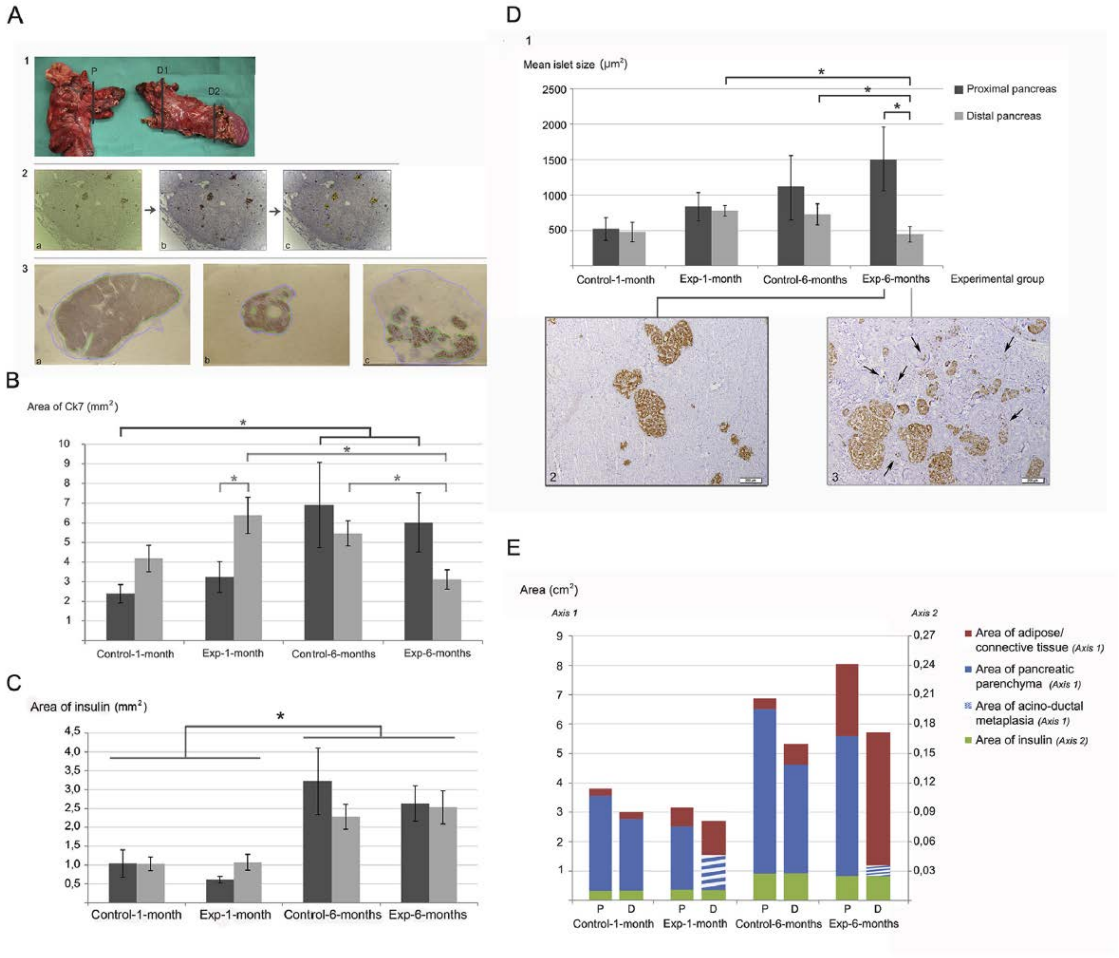

Figure 2. Quantitative methodology and results. **(A)** Schematic representation of the method applied. A-1) Area of analysis: "P" proximal, "D1" 1-2 cm next to the margin of transection, and "D2" next to the tail. A-2) Quantification of insulin with Micro-manager software: Appearance of the image after acquisition (A-2a), application of automatic contrast (A-2b) segmentation of the region of interest (ROI) (yellow, A-2c) and ROI manager (A-2d). A-3) Macroscopic study of the cross-section with 3D-DOCTOR for preparations "P" (A-3a), "D1" (A-3-b) and "D2" (A-3d) at 6 months PO (blue: total area, green: area of pancreatic parenchyma). **(B)** Area of Ck7 expression (mm^2) for experimental group and pancreatic section**. (C)** Area of I expression (mm^2) for experimental group and pancreatic section. **(D)** Mean islet size (μm^2) per experimental group and pancreatic section. Insulin IHC at 6 months PO from the proximal (D-2) and distal pancreas (D-3) (Arrows: positive isolated of β-cell clusters). (D) Tissue distribution of the cross-sectional pancreatic area, which includes the area of pancreatic parenchyma, acinar-to-ductal metaplasia, insulin and adipose/connective tissue. Values expressed as mean ± SD. Scale bar: 200 µm. *p<0.05.

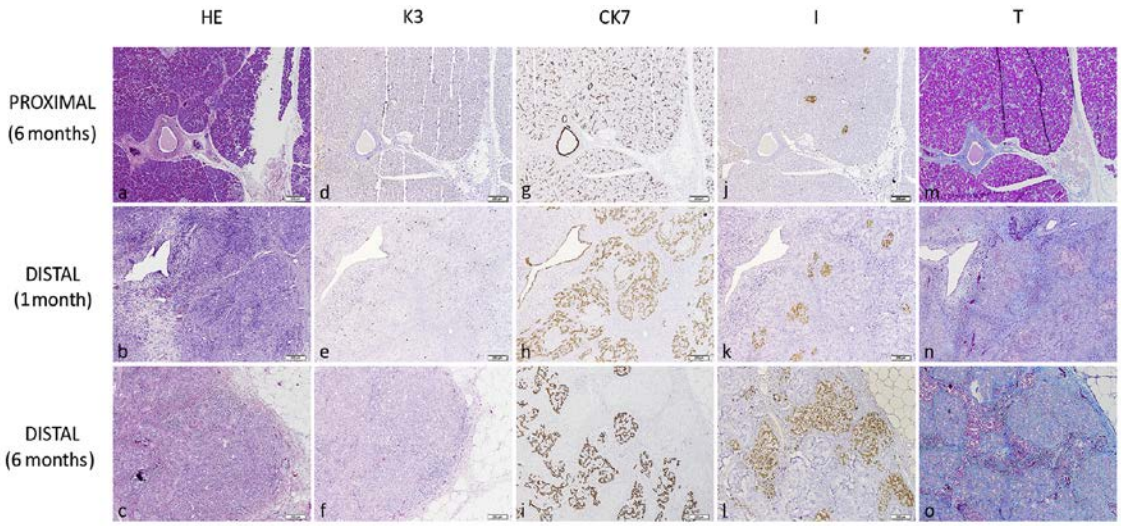

Figure 3. HE, immunohistochemical staining of caspase-3 (K3), citoqueratina-7 (CK7),insulin (I) and Masson Trichrome of the proximal pancreas at 6 months PO (a, d, g, j, m) and of the distal pancreas at one (b, e, h, k, n) and 6 months PO (c, f, i, l, o). No apoptotic activity was observed in the distal pancreas one and 6 months after surgery (e-f). CK7 expression in the wall of duct-like structures significantly increased in the distal pancreas a month after the surgery and remained high at 6 months (h-i), but seemed to be replaced by fibrotic tissue at 6 months (o). Insulin expression was observed in the proximal and distal pancreas at one and 6 months PO (j, k, l).

Table 1. Preoperative and postoperative amylase (peritoneal and serum) and glucose levels by group and throughout the postoperative period. Data expressed as mean±SEM. *p<0.05 throughout the postoperative period. **No peritoneal liquid was observed 6 months after the procedure.

	Postoperatory							
	Preoperatory	4 h	3 days	7 days	15 days	21 days	1 month	6 months
Amylase serum (U/L)	1363 ± 143	1916 ± 235*	2565 ± 834*	1814 ± 668	1083 ± 96	1201 ± 103	882 ± 113	1715 ± 119
Glucose serum (mg/dl)	126 ± 18	158 ± 15	152 ± 14	111 ± 4	127 ± 12	120 ± 8	146 ± 30	100 ± 8
Amylase peritoneal liquid (U/L)	476 ± 141	–	4234 ± 1079*	–	–	–	685 ± 131	**